

Author's Accepted Manuscript

Electrochemical impedance spectroscopy of enhanced layered nanocomposite ion exchange membranes

Carolina Fernandez-Gonzalez, John Kavanagh, Antonio Dominguez-Ramos, Raquel Ibañez, Angel Irabien, Yongsheng Chen, Hans Coster



www.elsevier.com/locate/memsci

PII: S0376-7388(17)30806-2
DOI: <http://dx.doi.org/10.1016/j.memsci.2017.07.046>
Reference: MEMSCI15451

To appear in: *Journal of Membrane Science*

Received date: 21 March 2017
Revised date: 27 June 2017
Accepted date: 21 July 2017

Cite this article as: Carolina Fernandez-Gonzalez, John Kavanagh, Antonio Dominguez-Ramos, Raquel Ibañez, Angel Irabien, Yongsheng Chen and Hans Coster, Electrochemical impedance spectroscopy of enhanced layered nanocomposite ion exchange membranes, *Journal of Membrane Science* <http://dx.doi.org/10.1016/j.memsci.2017.07.046>

This is a PDF file of an unedited manuscript that has been accepted for publication. As a service to our customers we are providing this early version of the manuscript. The manuscript will undergo copyediting, typesetting, and review of the resulting galley proof before it is published in its final citable form. Please note that during the production process errors may be discovered which could affect the content, and all legal disclaimers that apply to the journal pertain

Electrochemical impedance spectroscopy of enhanced layered nanocomposite ion exchange membranes

Carolina Fernandez-Gonzalez^{a,b,c*}, John Kavanagh^c, Antonio Dominguez-Ramos^a,
Raquel Ibañez^a, Angel Irabien^a, Yongsheng Chen^b, Hans Coster^c

^aDepartamento de Ingenierías Química y Biomolecular, ETS Ingenieros Industriales y de Telecomunicación, Universidad de Cantabria, Avda. Los Castros, s.n., Santander, 39005, Spain

^bSchool of Civil and Environmental Engineering, Georgia Institute of Technology, Atlanta, Georgia, 30332, USA

^cSchool of Chemical and Biomolecular Engineering, The University of Sydney, Sydney, NSW 2006, Australia

*Corresponding author. Tel.: +34942206778. carolina.fernandez@unican.es

Abstract

This work presents the enhancement of $\text{Cl}^-/\text{SO}_4^{2-}$ mono-selectivity of layered nanocomposite anion exchange membranes (AEMs) and the mechanism that supports this improvement. These nanocomposite membranes are based on commercial polyethylene AEMs and a nanocomposite negative thin layer composed of sulfonated poly (2,6-dimethyl-1,4-phenylene oxide) and a functionalized nanomaterial, $\text{Fe}_2\text{O}_3-\text{SO}_4^{2-}$ nanoparticles or oxidized multi-walled carbon nanotubes CNTs-COO⁻. The mechanism for monovalent selectivity was confirmed by characterizing nanocomposite membranes and commercial heterogeneous ion exchange membranes (IEMs) using ζ -potential and electrochemical impedance spectroscopy (EIS). ζ -potential measurements confirmed the modification of the charge of surface of the membrane after being coated with the nanocomposite layer. EIS measurements showed a totally different

electrical performance between layered nanocomposite membranes and commercial IEMs. The electrical data from EIS was fitted to a Maxwell-Wagner model providing an equivalent electric circuit (EEC) for each membrane. The observed differences in ECC were related to the structural differences of the membranes. A physical explanation of the phenomena that caused these differences is provided. The influence of ion concentration on EIS measurements was also studied. To the best of our knowledge, this is the first time that an ECC related to the structure of advanced layered IEMs is proposed.

1. Introduction

Surface modification of ion exchange membranes (IEMs) is one of the most promising techniques used to improve the performance of multilayered membrane systems [1]. The addition of a layer on the top of IEMs allows the modification of some properties of the membrane surface, which influence the membrane performance in terms of selectivity and fouling resistance. A relevant property of anion exchange membranes (AEMs), in order to avoid scaling and obtain higher purity products (such as HCl in electrodialysis with bipolar membranes), is the monovalent selectivity $\text{Cl}^-/\text{SO}_4^{2-}$ [2][3]. Traditionally, the permselectivity of AEMs for specific anions has been improved by increasing their degree of cross-linking, forming a tight layer on their surface, modifying their hydrophilicity, using photo-irradiation and including photo-responsive groups as well as imparting thermal sensitivity [3]. One simple and widely used method for membrane modification is the direct coating of membranes by chemical or electrostatic interaction at the membrane surface [4]. A significant number of studies have reported improvements in the $\text{Cl}^-/\text{SO}_4^{2-}$ selectivity by increasing the surface hydrophobicity of AEMs [5–8]. This is a well-known effect that happens as a result of the differences in the Gibbs hydration energy between the Cl^- ($317 \text{ kJ}\cdot\text{mol}^{-1}$) and SO_4^{2-} ($1,000 \text{ kJ}\cdot\text{mol}^{-1}$) [5]. In this way a hydrophobic membrane surface will facilitate the flux of the more hydrophobic anions, which in this case is Cl^- . However, membranes with a hydrophobic surface are not as effective in preventing fouling as membranes with a hydrophilic surface [9]. An increase in membrane surface hydrophilicity reduces the hydrophobic interactions of foulants with the membrane surface [10].

Recent studies have been focused on the surface modification of AEMs by adding a negative hydrophilic layer in order to improve their monovalent selectivity. The techniques used to add this layer were layer by layer deposition [11][12], immersion [13], and direct casting [14]. This negative layer will restrict the passage of divalent ions and will allow the passage of monovalent ions. This restriction is based on larger electrostatic repulsions between multivalent ions and the membrane surface than in the case of monovalent ions [15]. Thus the introduction of a negative hydrophilic layer on the surface of AEMs should confer on the membranes a simultaneous improvement of monovalent selectivity and fouling resistance.

Understanding the ionic processes involved in layered membranes is fundamental in order to achieve an adequate trade-off between selectivity and conductivity [1,16]. Electrical impedance spectroscopy (EIS) can be used as a method to characterize electrochemical processes with IEMs [17] as it allows a quantitative analysis of the internal “structure” of systems as components or “layers” described by electrical equivalent circuits (ECC) [18]. Traditionally, the electrical data obtained when IEMs were characterized by EIS were fitted to an ECC composed of three layers: specifically, the membrane structure itself, the electric double layer and the diffusion boundary layer [17–21]. Other examples report the fitting to more complex ECC [22,23]. However, most of the published work has been focused on the characterization of monopolar IEMs.

To the best of our knowledge, only a few studies in the literature deal with the characterization of complex systems with layered IEMs by EIS [1,24,25]. The first work [24] is a theoretical approach based on irreversible thermodynamics. The second study [1] simulates the effect of several multilayered membrane properties such as layer thickness on the EIS response of the system. However, neither physical interpretation nor ECC was presented in order to describe the electrical performance of multilayer membranes. The third study [25] is an experimental work in which multilayer cation exchange membranes were synthesized using layer by layer deposition. However, the ECC proposed to describe the electrical performance of the multilayer membranes was the same as the traditional one used for monopolar IEMs, which included three layers corresponding to the membrane, the diffusion boundary layer and the ionic double layer. A new approach is necessary to take into account the new interfaces generated in layered systems in order to understand their role in EIS.

In our previous studies [16,17], the authors modified one of the faces of commercial polyethylene AEMs with a negatively charged nanocomposite layer containing iron oxide nanoparticles or carbon nanotubes. This treatment improved the membrane fouling resistance, which translated into important savings in energy consumption [16]. These promising layered membranes also showed an outstanding stability when working with strong acids and bases [17]. The present study presents the results of $\text{Cl}^-/\text{SO}_4^{2-}$ selectivity of these nanocomposite membranes using ζ -potential and EIS measurements to provide evidence of the mechanism that underlies the observed monovalent selectivity. To the best of our knowledge, this is the first time that quantitative data obtained from EIS is used to elucidate this mechanism. This study compares applying EIS to layered nanocomposite AEMs with conventional heterogeneous AEMs and CEMs. A physical explanation for the different layers of the proposed ECC was also provided in each case. Moreover, the influence of solution ion concentration on the response of the membranes in EIS is presented and discussed. In our proposed ECC, the new interface generated at the junction between the nanocomposite layers and the AEMs is taken into account. This ECC and the physical phenomena associated with each layer shed light on the electric nature of advanced

layered membranes where negative layers and positive layers generate new interfaces, as is the case of the nanocomposite membranes studied in the present work.

Experimental

2.1. Materials

Commercial polyethylene AEMs RALEX AM-PP and CEM CM-PP (Mega, Czech Republic) were used for the permselectivity experiments and for the comparison of their ζ -potential and EIS measurements with nanocomposite AEMs. AM-PP membranes were subjected to modification to obtain the desired nanocomposite membranes. Poly (2,6-dimethyl-1,4-phenylene oxide) (PPO) (analytical standard grade), chloroform (anhydrous, 99wt%), methanol (anhydrous, 99.8wt %), chlorosulfonic acid (99wt%) and sulfuric acid (98wt%) were purchased from Sigma Aldrich (St. Louis, USA). Dimethyl sulfoxide (DMSO) (ACS grade, 99.9wt%), sodium chloride (99wt %) and sodium sulfate (anhydrous, < 99%) were purchased from VWR (Atlanta, USA). Iron (III) oxide nanoparticles ($\text{\O}50\text{nm}$, Sigma Aldrich, USA) were subjected to sulfonation. Oxidized multi-walled carbon nanotubes were obtained from Cheap Tubes (Cambridge, USA) (purity 95wt%, carboxyl group content 3.86 wt%, diameter lower than 8 nm, length $10\mu\text{m}$ – $30\mu\text{m}$) and used as received.

2.2. Nanocomposite membranes

Two types of nanocomposite membranes were used in this work. Nanocomposite membranes containing functionalized iron oxide nanoparticles $\text{Fe}_2\text{O}_3\text{-SO}_4^{2-}$ or oxidized multi-walled carbon nanotubes CNTs-COO^- . These membranes were obtained by direct coating of commercial polyethylene AEM AM-PP with sulfonated PPO (sPPO) and the selected nanomaterial. The dose of nanomaterial in the coating ranged from $0.2\% \text{ g}\cdot\text{g}^{-1}$ to $0.6\% \text{ g}\cdot\text{g}^{-1}$ of $\text{Fe}_2\text{O}_3\text{-SO}_4^{2-}$ and from $0.2\% \text{ g}\cdot\text{g}^{-1}$ to $0.8\% \text{ g}\cdot\text{g}^{-1}$ of CNTs-COO^- . PPO and Fe_2O_3 nanoparticles were sulfonated using chlorosulfonic acid as the sulfonating agent and chloroform and methanol as solvents following the procedure described in [26,27]. AM-PP membranes were modified using the doctor blade method and the solvent evaporation technique. In order to control the uniformity of the thickness of nanocomposite thin-film, special attention was given to the thickness selected in the doctor blade and the quantity of solvent added to dissolve the polymer and the nanomaterials, as the viscosity of the final solution coating the commercial AEMs plays a key role in the final layer uniformity and thickness. Additional information about membrane pretreatment before modification, drying process and membrane post-treatment can be found in our previous work [28].

Only one of the sides of AM-PP membranes was subjected to modification because: a) the monovalent selectivity of membranes is mainly determined by the layer facing the dilute compartment [13], thereby forming a barrier for SO_4^{2-} ions in the direction of the flux of anions (from dilute to concentrate compartments as shown in Figure 1); and b) the modification of both sides of the membrane might potentially decrease Na^+/Cl^-

permselectivity of AEMs due to an increase of the interactions between Na^+ cations and the negatively charged membrane surface in the side facing the concentrate compartment [28]. This can be avoided if only the side facing the dilute compartment is modified (see Figure 1).

Table 1 includes a summary of the seven nanocomposite membranes used in this work. These membranes already showed a promising fouling resistant [28], and in the case of the membranes containing $\text{Fe}_2\text{O}_3\text{-SO}_4^{2-}$, also showed a good stability in valorization of desalination brines into acids and bases by electrodialysis with bipolar membranes[29].

Table 1. Summary of nanocomposite ion exchange membranes used in this work.

Membrane code	Nanocomposite layer	Loading of nanomaterial (% $\text{g}\cdot\text{g}^{-1}$ *)
AM-0.2NP	SPPO, $\text{Fe}_2\text{O}_3\text{-SO}_4^{2-}$	0.2
AM-0.4NP	SPPO, $\text{Fe}_2\text{O}_3\text{-SO}_4^{2-}$	0.4
AM-0.6NP	SPPO, $\text{Fe}_2\text{O}_3\text{-SO}_4^{2-}$	0.6
AM-0.2CNTs	SPPO, CNTs-COO^-	0.2
AM-0.4CNTs	SPPO, CNTs-COO^-	0.4
AM-0.6CNTs	SPPO, CNTs-COO^-	0.6
AM-0.8CNTs	SPPO, CNTs-COO^-	0.8

*g nanomaterial \cdot g^{-1} layer.

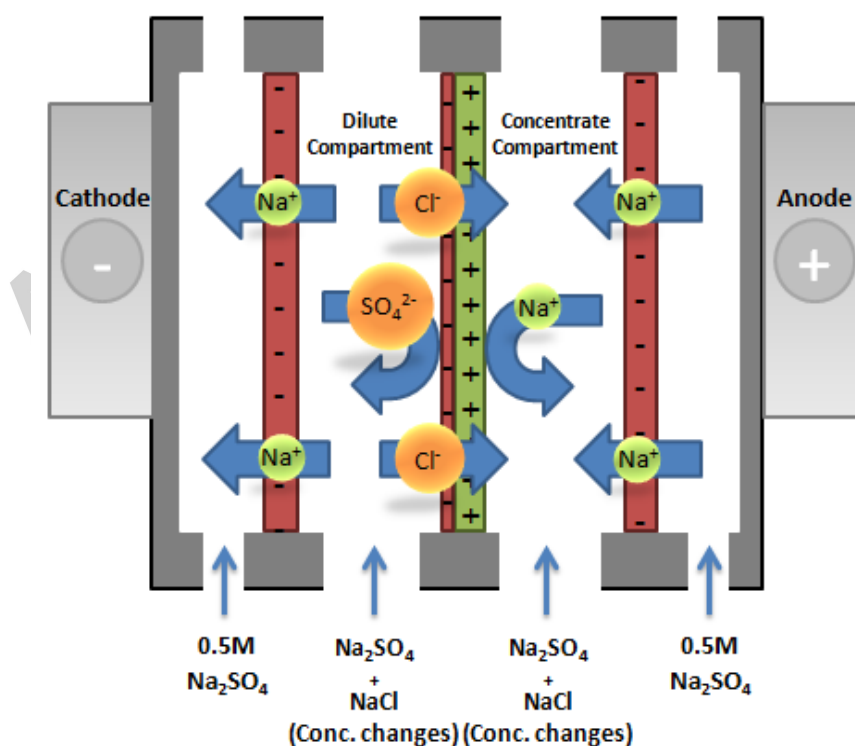


Fig 1. Scheme of the experimental setup used for the permselectivity experiments and mechanism of monovalent ion selectivity of the nanocomposite anion exchange membranes.

2.3. Analysis of the monovalent ion permselectivity

The monovalent selectivity of AEMs was calculated from the comparison of the transport number of Cl^- and SO_4^{2-} in the dilute compartment. The transport number for an ion t_A can be defined as the ratio between the flux of the ion (J_A) and the total flux of ions (J_T) [29]:

$$t_A = \frac{J_A}{J_T} \quad \text{Eq. 1}$$

To evaluate the relative permselectivity of the membranes between different ions, in this case Cl^- and SO_4^{2-} , and avoid the mole fraction effect [3,12], the transport number ratio can be defined as:

$$P_{\text{SO}_4/\text{Cl}} = \frac{t_{\text{SO}_4}/t_{\text{Cl}}}{C_{\text{SO}_4}/C_{\text{Cl}}} = \frac{J_{\text{SO}_4}/J_{\text{Cl}}}{C_{\text{SO}_4}/C_{\text{Cl}}} \quad \text{Eq. 2}$$

Where $P_{\text{SO}_4/\text{Cl}}$ is the permselectivity $\text{SO}_4^{2-}/\text{Cl}^-$. According to this definition, the lower the $P_{\text{SO}_4/\text{Cl}}$, the higher the monovalent selectivity of AEMs. Permselectivity experiments were carried out in the four-compartment ED cell shown in Figure 1. The modified surface of the membrane was set facing the dilute compartment as previously mentioned. The effective area of the cell was 100 cm^2 , and the applied current density was $12 \text{ mA}\cdot\text{cm}^{-2}$. This current density was also used in the permselectivity determination of our previous study [29]. A solution of NaCl and Na_2SO_4 , each with a concentration of $0.05 \text{ mol}\cdot\text{L}^{-1}$, was fed to the dilute and concentrate compartment. A solution $0.5 \text{ mol}\cdot\text{L}^{-1}$ of Na_2SO_4 was used as an electrolyte solution in the electrode compartment. These solutions were pumped into the cell at a rate of $40 \text{ L}\cdot\text{h}^{-1}$. The concentration of Cl^- , SO_4^{2-} and Na^+ was determined by ion chromatography (Dionex ICIS-1100 for anions and Dionex DX-120 for cations, Dionex Corp., USA). The flux of Cl^- , SO_4^{2-} and Na^+ were calculated from the evolution of their concentration in the dilute compartment.

2.4. Determination of the mechanism for monovalent selectivity

A combination of ζ -potential and impedance measurements was used to confirm the mechanism for the monovalent selectivity of nanocomposite membranes and to compare their electrical behavior with the unmodified AEMs and CEMs. ζ -potential measurements gave information of membrane surface charges. This information was related to the impedance observed using EIS. Impedance measurements were fitted to a Maxwell-Wagner model to identify and understand the phenomena happening in the system in the presence of an alternating current. This fitting was then related to structural differences between unmodified IEMs and nanocomposite AEMs.

2.4.1 ζ - potential

A SurPASS electro-kinetic analyzer UAnton (Anton Paar, Barcelona; Spain) was used to measure the streaming potential and determine the ζ - potential of the membranes using a solution $0.01 \text{ mol}\cdot\text{L}^{-1}$ of NaCl at room temperature.

2.4.2 Electrochemical impedance spectroscopy

The electrical characterization of unmodified IEMs and nanocomposite layered AEMs was done using EIS in a two-compartment chamber with an effective membrane area of 3.80 cm^2 using solution concentrations $0.01 \text{ mol}\cdot\text{L}^{-1}$ of NaCl, $0.05 \text{ mol}\cdot\text{L}^{-1}$ of NaCl, $0.1 \text{ mol}\cdot\text{L}^{-1}$ of NaCl and $0.5 \text{ mol}\cdot\text{L}^{-1}$ of NaCl. The impedance was measured with a high resolution impedance spectrometer from INPHAZE (Sydney, Australia) using a 4-terminal method. The 4-terminal method ensures that the frequency dependent impedance of the solution-electrode interface does not affect the measurement of the impedance of the membrane system. The signal appearing across the membrane was kept to an amplitude below 30 mV to minimize the effects of non-linearities. The impedance spectrometer has a phase resolution of 0.001 degrees and a precision of 0.001% for impedance, which is important for measuring the capacitance of the membranes with a high degree of precision, particularly at very low frequencies [30–32]. The impedance measurements were performed over frequencies from 0.112 Hz to 1831.055 Hz.

2.4.2.1 The Maxwell-Wagner model

The impedance of a system Z is defined as the relationship between the alternating voltage (AC) applied across a sample to the current flowing through it. This impedance can be expressed as a complex number in terms of an equivalent parallel combination of a conductance G and a capacitance C , and is a function of the angular frequency ω , as expressed in Eq. 3.

$$Z = \frac{1}{G + j\omega C}, \quad \text{where } j^2 = -1 \quad \text{Eq. 3}$$

The Maxwell-Wagner model describes a system composed of several electrically different regions or layers in series and the total impedance of the system Z is then the sum of the individual Z_k impedances of each of the k layers [31]. Thus, the impedance of the total system Z can be expressed as a function of the conductance G_k and capacitance C_k of each of the k layers using Eq. 4 as follows:

$$Z = \sum_{k=1}^K Z_k = \sum_{k=1}^K \frac{1}{G_k + j\omega C_k} \quad \text{Eq. 4}$$

The Maxwell-Wagner model can be represented by the electrical circuit shown in Figure 2. Although the conductance G_k and capacitance C_k of each layer are independent of the angular frequency ω , it should be noted that the capacitance and conductance of the total system will depend on the angular frequency ω . Indeed, the dependence on frequency of the total impedance allows the values of the capacitances and conductances of the various layers to be determined.

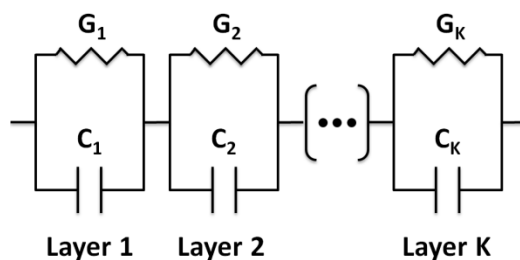


Fig 2. Electrical circuit representing a system made of k electrically different layers using the Maxwell-Wagner model.

The fitting of the impedance obtained by EIS to the Maxwell-Wagner model was done using a commercial software package from INPHAZE (EIS Impedance Structure Refinement version 1.16.515). With this software, it is not required to specify the number of layers in the Maxwell-Wagner model. Instead, the software sequentially adds additional layers in order to reduce the χ^2 error between the model and measured data but only until the *Reduced* χ^2 reaches a minimum value. The fit and the number of layers introduced is thus statistically significant, as the fitting routine also takes into account experimental errors (standard errors from the mean in repeated measurements, see also [32]). Therefore, the selection of a number of layers is statistically supported.

3. Results and discussion

3.1 Analysis of monovalent ion permselectivity

AEMs are commonly more selective to divalent anions than monovalent anions as the electrostatic interactions between the positively charged surface of AEMs and divalent anions are stronger [15]. In this work, the monovalent selectivity of AEMs was evaluated by comparing the transport numbers of SO_4^{2-} and Cl^- using Eq.1 and Eq.2. Ionic fluxes of anions were calculated from the evolution of its concentration in the dilute compartment. Table 2 includes the permselectivity sulfate/chloride ($P_{\text{SO}_4/\text{Cl}}$) of commercial and nanocomposite membranes. Since permselectivity is defined as the ratio between the transport number of sulfate (t_{SO_4}) and the transport number of chloride (t_{Cl}) divided by the ratio of the averaged concentration of both species in the dilute compartment, the lower the transport number, the better the monovalent selectivity.

The permselectivity data included in Table 2 shows a significant enhancement of monovalent selectivity in all the nanocomposite membranes. This enhancement ranged from 26% to 34%. The best nanocomposite membranes AM-0.4NP and AM-0.6CNTs showed a significant improvement in terms of $\text{Cl}^-/\text{SO}_4^{2-}$ selectivity when compared with a previous study [14] in which AEMs were modified by casting (AM-0.4NP and AM-0.6CNTs showed a 34% improvement compared to a 10% improvement in [14]).

Table 2. Summary of transport numbers for chloride and sulfate in commercial and nanocomposite anion exchange membranes.

Membrane	t_{Cl}	t_{SO_4}	$P_{SO_4/Cl}$	Permselectivity improvement (%)
Commercial	0.478	0.522	1.08±0.15	-
AM-0.2NP	0.525	0.475	0.81±0.01	33
AM-0.4NP	0.528	0.472	0.81±0.01	34
AM-0.6NP	0.514	0.486	0.86±0.01	26
AM-0.2CNTs	0.504	0.496	0.89±0.03	21
AM-0.4CNTs	0.516	0.484	0.844±0.01	28
AM-0.6CNTs	0.525	0.477	0.806±0.01	34
AM-0.8CNTs	0.532	0.468	0.817±0.02	32

Besides the monovalent selectivity, all nanocomposite membranes presented a higher flux of Cl^- than the unmodified membrane AM-PP. Figure 3 includes a summary of permselectivity and flux improvement for each nanocomposite membrane. The flux of Cl^- increased with the load of $Fe_2O_3-SO_4^{2-}$ nanoparticles and oxidized multi-walled carbon nanotubes CNTs-COO⁻ in membranes. A maximum enhancement of 17.4% was achieved. Nanocomposite membranes modified with iron oxide nanoparticles showed a slightly higher Cl^- flux than the modified using CNTs. Previous studies [14] reported a modest increase of 2.6% in the flux of Cl^- when a commercial AEM was modified with a negative coating. The enhancement of the flux by up to 17.4% in the present study might be attributable to the presence of the two nanomaterials in a homogeneous, very thin and highly ion-conductive nanocomposite film.

The 0.4% load of functionalized iron oxide nanoparticles was selected as the optimum for the nanocomposite thin layer, as it enhanced simultaneously the monovalent selectivity and the Cl^- flux of the unmodified membrane by 34.1% and 15.2%, respectively (see Figure 3). In the case of the membranes modified with CNTs, a slightly higher loading of 0.6% was selected as the optimum with an improvement of 34.0% in monovalent selectivity and 11.5% in Cl^- flux. This is a significant advance regarding the work already published about modification of AEMs for higher monovalent selectivity as it significantly boosts not only the Cl^-/SO_4^{2-} selectivity but also the Cl^- flux. To the best of the authors' knowledge, this enhancement has not been reported before, neither in the studies that modify the membrane by increasing hydrophobicity nor in those which add a negative layer to the surface.

Additionally, no loss of Na^+/Cl^- permselectivity was observed, probably because the commercial membrane was only modified on one of its sides (Figure 1), keeping the original positive charge of the commercial AEM in the side facing the anode.

It is worth mentioning that the optimum loading observed in this study for both nanomaterials (0.4 wt% for NP and 0.6 wt% for CNTs) is the same as the one observed in our previous study on fouling resistance of nanocomposite membranes [28]. The improvement using CNTs and NP was very similar in terms of monovalent selectivity and Cl^- flux for a very similar loading of nanomaterial. This supports the hypothesis that different nanomaterials with totally different geometries and functional groups, such as the CNTs-COO⁻ and NP-SO₄²⁻ used in this study, can give the same performance not only in terms of fouling resistance [28] but also in terms of ion transport. Qualitative and quantitative evidence are provided here in and discussed to

support a mechanism that explains the difference of the performance observed on modifying commercial AEMs with a negative nanocomposite film.

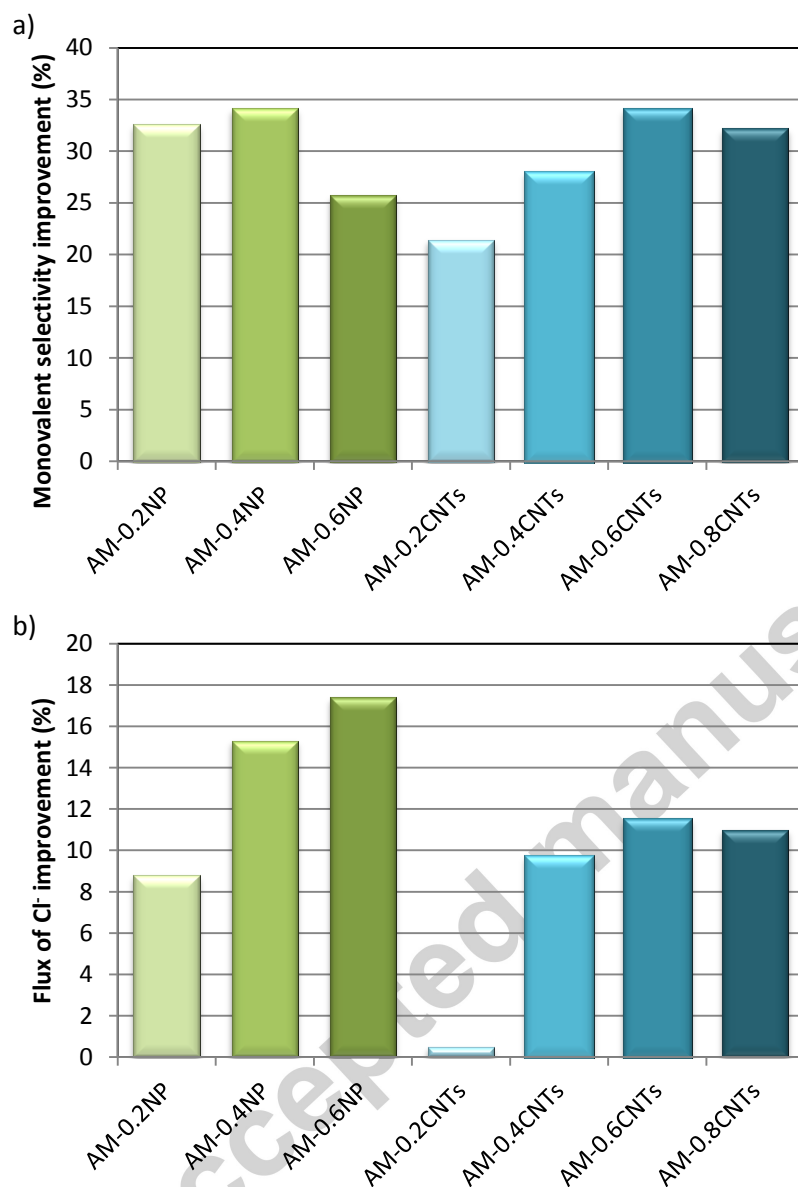


Fig 3. Improvement of a) monovalent permselectivity and b) flux of Cl⁻ of nanocomposite membranes versus unmodified membranes AM-PP.

3.2 Determination of the mechanism for monovalent selectivity

3.2.1 ζ - potential

ζ -potential describes the interactions of charged surfaces with their surroundings [12], and it is used to evaluate the surface charge distribution of IEMs [17]. Figure 4 includes the measurements of the ζ -potential of the commercial IEMs used in this work, CM-PP and AM-PP, and the best nanocomposite AEMs, AM-0.4NP and AM-0.6CNTs.

Commercial IEMs such as the heterogeneous CEMs CM-PP presented a ζ -potential of -20mV while the AEMs AM-PP had a ζ -potential of 10 mV . The difference in the absolute value of the ζ -potential between the two membranes is due to the higher ion exchange capacity (IEC) of CM-PP membranes[33]. Higher ion fluxes, pointing to a higher IEC of CM-PP, were observed in our previous work [29]. The increased density of ion exchange groups on the membrane surface then led to a higher absolute value of the ζ -potential. The nanocomposite AEMs AM-0.4NP and AM-0.6CNTs had the same ζ -potential of -10V . The treatment of AEMs AM-PP with the nanocomposite layer successfully changed the membrane surface charge from 10 mV to -10 mV . This was translated into an enhancement of monovalent selectivity, as presented in section 3.1 *Analysis of monovalent ion permselectivity*. The enhancement was related to the increase of the electrostatic repulsions between sulfate ions and the membrane surface. Similarly a negative ζ -potential of around -10 mV was reported when using layer-by-layer deposition as a modification technique of commercial AEMs[12].

The ζ -potential values obtained for the heterogeneous IEMs, AM-PP and CM-PP, are much lower than reported for other homogeneous IEMs in the literature (ζ -potential of AEMs 65.6 mV to 82.3 mV and CEM -80.9 mV to -90.4 mV [17]). This difference in surface charge will have a great influence in the electrochemical characterization of the IEMs by EIS, as will be discussed in section 3.2.2 *Impedance of IEMs: Differences between unmodified and layered nanocomposite membranes and fitting to the Maxwell-Wagner model*.

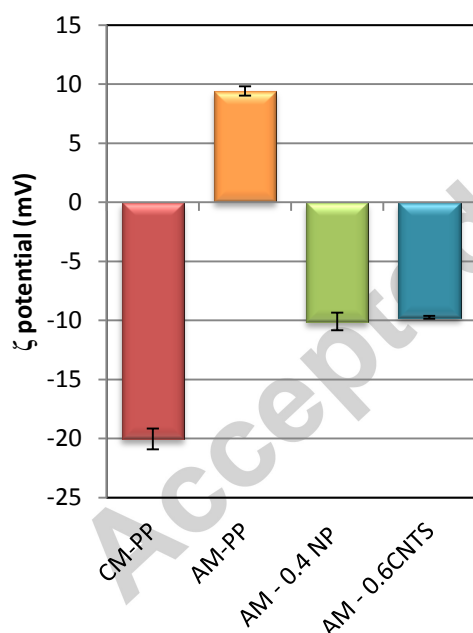


Fig 4. ζ potential of commercial ion exchange membranes CM-PP (CEM) and AM-PP (AEM) and nanocomposite AEMs AM-0.4NP and AM-0.6CNTs.

3.2.2 Impedance of IEMs: Differences between unmodified and layered nanocomposite membranes and fitting to the Maxwell-Wagner model.

EIS is a powerful tool for the characterization of systems with IEMs as it allows characterization of the substructural layers with different electrical time constants within

the system [21,32]. Additionally, unlike other membrane characterization techniques that only provide qualitative information, EIS provides quantitative information about the different sublayers, such as conductance and capacitance, which is very useful in being able to understand the complex phenomena occurring in systems working with IEMs.

Figure 5 includes the variation of the impedance, capacitance, and phase with frequency for the unmodified heterogeneous IEMs AM-PP and CM-PP and the selected nanocomposite membranes AM-0.4NP and AM-0.6CNTs in a solution $0.01 \text{ mol}\cdot\text{L}^{-1}$ of NaCl. Unmodified membranes and nanocomposite membranes presented a totally different spectra from each other. The impedance of the unmodified heterogeneous membranes, AM-PP and CM-PP, were largely independent of frequency in the range of frequencies from 0.1 Hz to 1,000 Hz. The phase shift was almost zero over this entire range and hence the measured capacitance was negligible. Thus, when these heterogeneous IEMs are in solution, these systems behave as an electrically homogeneous material (system of only one layer), with a characteristic high conductance independent of frequency [31][32].

However, the impedance and capacitance of nanocomposite AEMs were frequency dependent, with a significant phase shift at low to medium frequencies (0.1 to 100 Hz, Figure 5c)). Phase differences in impedance measurements arise when the system is capable of storing charge [31]. Thus, the introduction of the negatively charged nanocomposite thin film on the surface of the AEMs, AM-PP, provides nanocomposite membranes with a capacitive character. The modification of spectral response in impedance and capacitance with frequency suggests that there is a substructure within the system that should be capable of being modeled using a Maxwell-Wagner model [32]. Thus the modification of AEMs with the thin negatively charged layer transforms the electrical behavior of the system from an electrical homogeneous monolayered system to a multilayered system.

The experimental EIS data were fitted to a Maxwell-Wagner (M-W) model using the INPHAZE Structure Refinement software. The results are shown in Figure 5. The continuous lines are the theoretical fits and the points represent the experimental data and error bars. Note the error bars are generally smaller than the size of the plot symbols used.

The fitting returned a single layer M-W structure for the unmodified AEM and CEM membranes, as was expected. However, for the nanocomposite AEMs, a 3-layer substructure was revealed. The same number of layers for each membrane was obtained for all the solution concentrations studied in this work ($0.01 \text{ mol}\cdot\text{L}^{-1}$ of NaCl, $0.05 \text{ mol}\cdot\text{L}^{-1}$ of NaCl, $0.1 \text{ mol}\cdot\text{L}^{-1}$ of NaCl and $0.5 \text{ mol}\cdot\text{L}^{-1}$ of NaCl, to be discussed in the next section). Regression parameters χ^2 and reduced χ^2 for all the fittings are included in Table S1 of the supplementary data.

One of the layers identified by the EIS is clearly the two membranes making up the composite. However, the EIS revealed the establishment of two additional layers and from an impedance point of view, very significant additional layers. The equivalent electric circuit (ECC) obtained from the fitting of the experimental data to the M-W model for the studied membranes is presented in Figure 6 and compared with the ECC reported in the literature for homogeneous AEM.

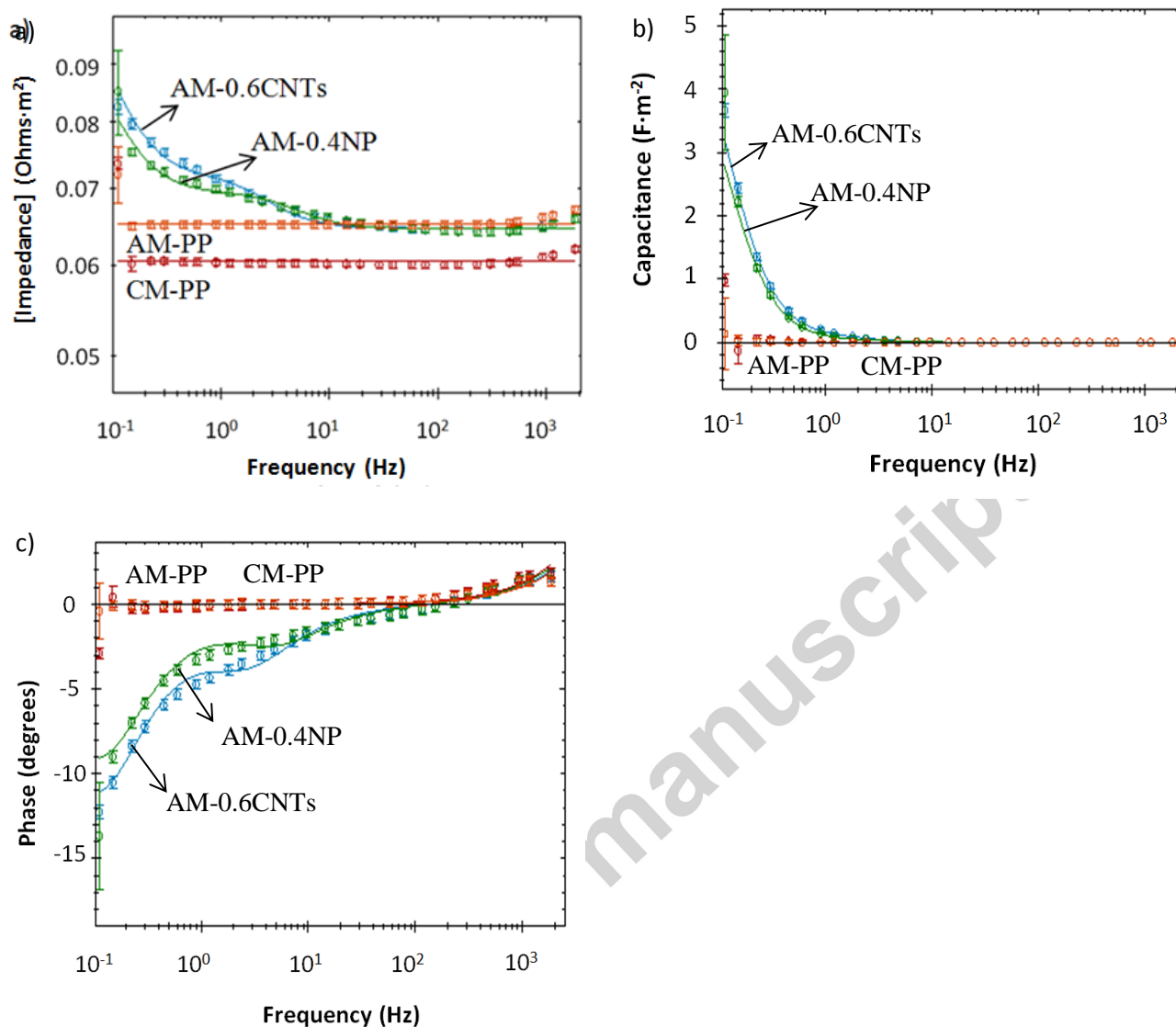


Fig 5. Dispersion of a) module of impedance, b) capacitance and c) phase with frequency for the membranes AM-PP \circ , CM-PP \circ , AM-0.4NP \circ and AM-0.6CNTs \circ . The solution was 0.01 M NaCl. The Maxwell-Wagner fitting of the experimental data is shown as continuous lines. The experimental results are for three consecutive complete EIS spectra; the error bars show least square error from the mean. The error bars are generally small.

Figure 6a) includes the phenomena widely reported in the literature for homogeneous IEMs in medium-high frequencies: a pure conductance corresponding to the membrane at high frequencies and a combination of conductance and capacitance corresponding to the double layer (DoL) at medium frequencies [21]. The DoL in AEMs is the layer formed at the interface between the membrane surface (positively charged) and the solution and it is due to the presence of positive fixed charges of the membrane and the profile of (negative) counter ions in the solution that compensate these fixed charges.

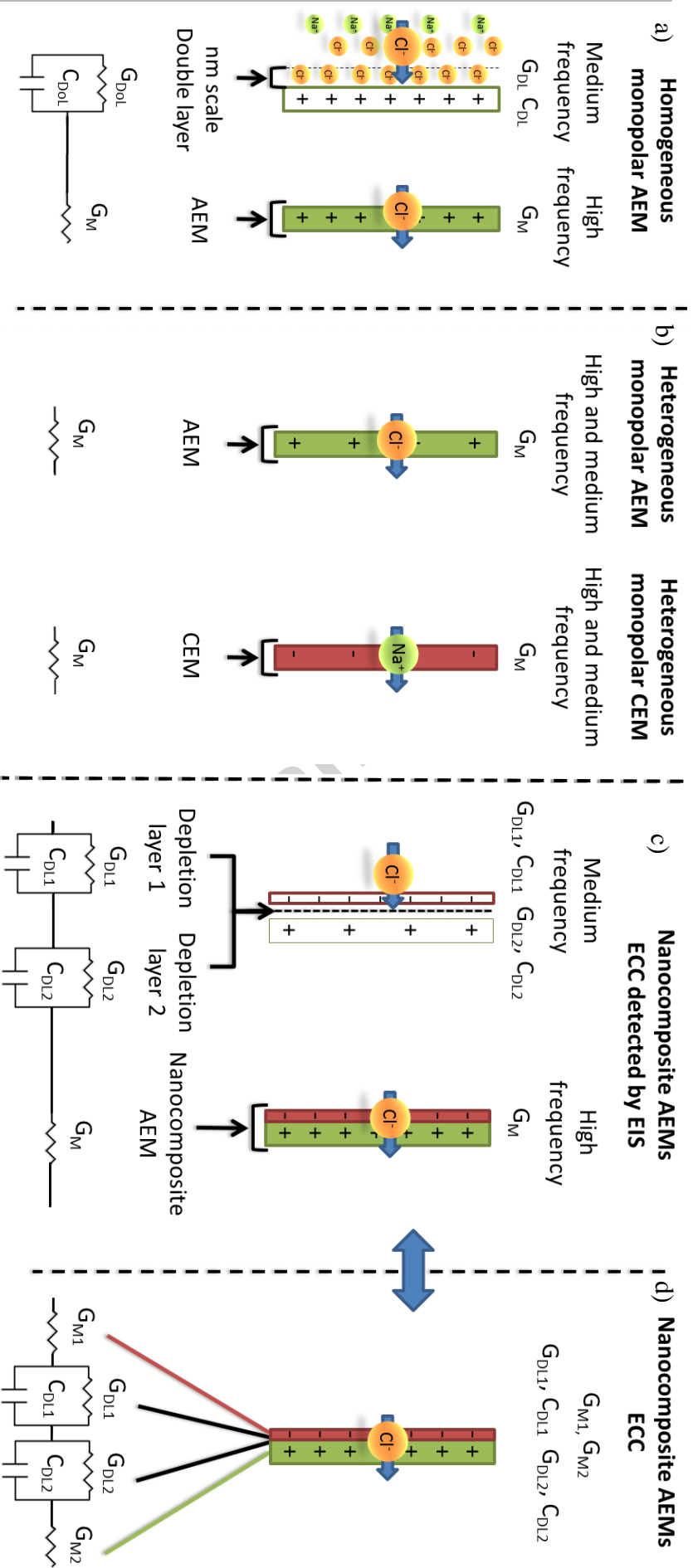


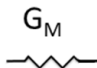
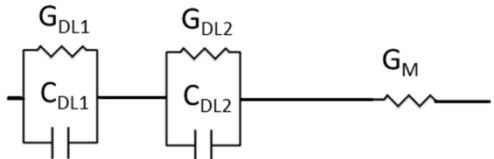
Fig 6. Summary of the equivalent electric circuit (EEC) of different IEMs for an alternating current in EIS. a) Homogeneous monopolar AEM (reported in [21]), b) heterogeneous monopolar AEMs and CEMs of this study and c) nanocomposite layered AEMs of this study. EIS cannot determine the order in which the layers are actually located. To assist in conceptualizing the ECC based on taking into account the known juxtapositioning and underlying physical behavior, the Maxwell-Wagner circuit equivalent has been redrawn in (d). Note that the conductance element G_M as shown in (c) is here shown as two elements, G_{M1} and G_{M2} , although the EIS can only determine their combined series value.

Figure 6b) includes the ECC proposed in this work for heterogeneous IEMs. In the two heterogeneous membranes characterized in this work, we only identified the membrane conductance at medium and high frequencies. This is probably due to the high content of PE on the surface of the heterogeneous IEMs as a consequence of their production process [34]. This high content of PE reduces the number of functional groups on the membrane surface, and thus, also the resistance of the double layer, as the resistance of the double layer is reported to decrease with the fixed charge density of the membrane surface [17]. The relatively low content of functional groups on the membrane was confirmed by the low ζ -potential of heterogeneous IEMs in comparison with other homogeneous IEMs characterized by EIS [17] (see section 3.2.1 ζ -potential). High hydrophobicity of the AEM AM-PP pointing to a high content of polyethylene on the membrane surface was also identified in our previous study [28].

Figure 6c) presents the ECC for the layered nanocomposite AEMs studied in this work. At high frequencies the system behaves as a pure conductance, while at medium frequencies, two additional layers contribute to the impedance of the system. The capacitances and conductances of the Maxwell-Wagner layer model fitted to the data (as shown in Figure 6) are set out in Table 3.

Table 3. Capacitances and conductances of the Maxwell-Wagner model fitting for different IEMs in a solution 0.01M of NaCl. The ECC of each membrane is also included.

Membrane	CM-PP	AM-PP	AM-0.4NP	AM-0.6CNTs
G_M ($S \cdot m^{-2}$)	1.66E+01	1.53E+01	1.55E+01	1.55E+01
G_{DL1} ($S \cdot m^{-2}$)	-	-	2.08E+02	1.43E+02
C_{DL1} ($F \cdot m^{-2}$)	-	-	6.72E+00	8.60E+00
G_{DL2} ($S \cdot m^{-2}$)	-	-	3.89E+01	3.00E+01
C_{DL2} ($F \cdot m^{-2}$)	-	-	6.90E+01	5.69E+01

ECC		
-----	---	--

In this work, we hypothesize that these two layers are two parts of the depletion layer generated at the interface between the positive and the negative region of nanocomposite membranes. DL1 is the part of the depletion layer formed within the negative region (nanocomposite layer), and DL2 is the part of the depletion layer formed within the positive region (AEM Ralex AM-PP). The concept of depletion layer has been applied to bipolar membranes in the past, being defined as a layer formed at the junction between a negatively charged region and a positively charged region in which the concentration of mobile ions (both anions and cations) is very low [35–37]. This depletion layer leads to the storage of charge in membranes and a capacitive character of the system under alternating currents [35][36].

A previous study [37] developed a model that describes the formation of depletion layers in bipolar membranes based on the Poisson equation and Maxwell-Boltzmann

distribution law. Eq. 5 and Eq. 6 are part of this model and relate electrostatic potential ψ with the widths of the depletion layer in the positive and the negative regions.

$$\psi_{\lambda_{N^-}}(x = \lambda_{N^-}) = \frac{q N^-}{2\varepsilon} \lambda_{N^-}^2 \quad \text{Eq. 5}$$

$$\psi_{\lambda_{N^+}}(x = \lambda_{N^+}) = \frac{q N^+}{2\varepsilon} \lambda_{N^+}^2 \quad \text{Eq. 6}$$

ψ ($x = \lambda_{N^-}$) is the electrostatic potential at the interface between the depletion layer and the negative region of the membrane. ψ ($x = \lambda_{N^+}$) is the electrostatic potential at the interface between the depletion layer and the positive region of the membrane, ε is the dielectric constant, and N^- is the density of negative fixed charges in the membrane. N^+ is the density of positive fixed charges in the membrane, q is the unit of electrical charge on fixed charges, λ_{N^-} is the width of the depletion layer in the negative region and λ_{N^+} is the width of the depletion layer in the positive region.

From Eq. 5 and Eq. 6 reported in [37], the thickness of the depletion layer in the two regions of the bipolar membrane can be related to two important parameters, the dielectric constant ε and the density of fixed charges (N^+ and N^-), also referred as IEC. For simplicity, Eq. 5 and Eq. 6 include the same dielectric constant for the two regions of the membrane. However, this dielectric constant could be significantly different as a function of the nature of the layers forming the membrane. Eq.7 and Eq. 8 include a variation of Eq. 5 and Eq. 6 taking into account that the dielectric constant of the negative region ε_{N^-} is not necessarily equal to the dielectric constant of the positive region ε_{N^+} .

$$\lambda_{N^-} = \sqrt{\frac{2 \varepsilon_{N^-} \psi_{\lambda_{N^-}}}{q N^-}} \quad \text{Eq. 7}$$

$$\lambda_{N^+} = \sqrt{\frac{2 \varepsilon_{N^+} \psi_{\lambda_{N^+}}}{q N^+}} \quad \text{Eq. 8}$$

The total electrostatic potential appearing across the depletion layers is thus;

$$\psi_T = \psi_{\lambda_{N^-}} + \psi_{\lambda_{N^+}} \quad \text{Eq. 9}$$

where $\psi_{\lambda_{N^-}}$ and $\psi_{\lambda_{N^+}}$ are the Donnan potentials between the solution and the negative and positive fixed charge phases respectively.

It should be noted here that apart from the classical Donnan effect of the fixed charges, ion partitioning from the solution into the fixed charge regions is not taken into account in Eq. 5–9. However, differences between the dielectric constant of the solution phase and ion exchange membrane will also lead to ion partitioning due to dielectric exclusion effects arising from the Born energy (defined later). The dielectric exclusion effect greatly enhances the electrostatic effects described by the usual Donnan equilibrium. Details of this effect on the depletion layers in bipolar membranes are described in Coster's 1973 seminal

work on solution-membrane ion partition effects [38], which showed that the limiting case for the Donnan equilibrium when the solution concentrations are low compared to the fixed charge density, remains valid, even when the external ion concentrations are higher than the fixed charge concentrations. Eq. 7 and Eq. 8 assume that the co-ion concentrations in each IEM are very small compared to the counter-ion concentration. Provided that the dielectric constant in the membranes are much smaller than that of the external solution, this is a valid assumption, even at high solution concentrations. The dielectric partition coefficient γ is given by:

$$\gamma = e^{-W/RT} \quad \text{Eq. 10}$$

where for monovalent ions of radius r , the Born energy W is given by:

$$W = \frac{F^2}{8\pi r} \left(\frac{1}{\epsilon_m} - \frac{1}{\epsilon_w} \right) \quad \text{Eq. 11}$$

where ϵ_m is the dielectric constant of the fixed charge phase and ϵ_w the dielectric constant of the solution.

As the dielectric constant of the fixed-charge phase increases, the Born energy partitioning effect decreases. This generally implies that the Donnan potentials will decrease unless the external electrolyte has a very low concentration. The partition coefficient and hence the Donnan potentials (verified by Eq. 7 and Eq. 8) show the depletion layers to be a sensitive function of the dielectric constant of the fixed charge phase.

For illustrative purposes, Figure 7 shows a qualitative profile of the concentration of mobile positive ions P and mobile negative ions N in a system formed by a bipolar membrane separating two identical solutions containing a concentration of positive ions P_s and a concentration of negative ions N_s . The concentration of positive and negative mobile ions in the membrane are P_m and N_m , respectively. Figure 7 also identifies various membrane parameters of Eq. 7 and Eq. 8, i.e., N^- , N^+ , ϵ_{N^+} , ϵ_{N^-} , λ_{N^+} and λ_{N^-} .

Bipolar membrane

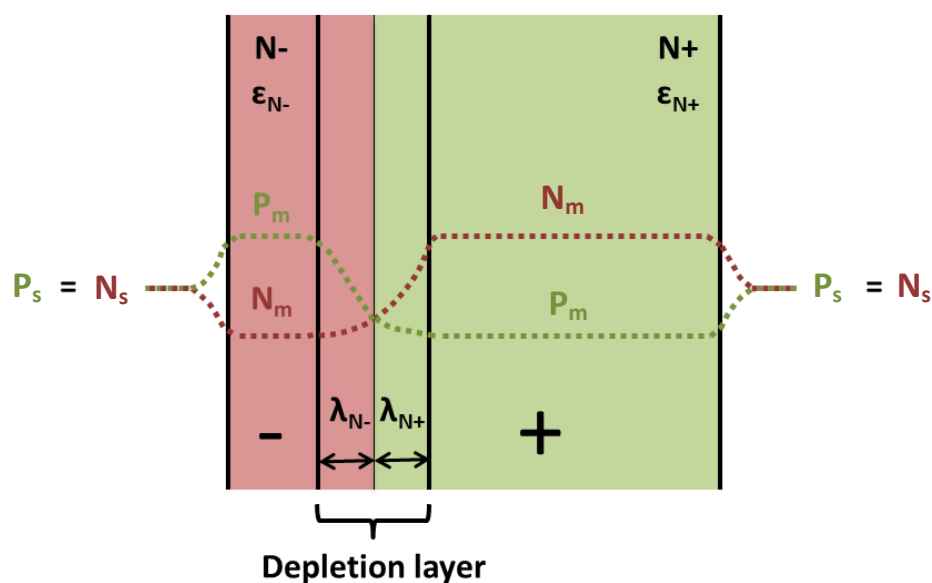


Fig 7. Qualitative profiles of the concentration of mobile positive ions P and mobile negative ions N in system formed when a bipolar membrane is separating two identical solutions.

According to Eqs. 7–11, two properties of the material forming the nanocomposite membranes have a significant influence over the thickness of the depletion layer generated in each membrane region: 1) the density of fixed ions, also referred as EIC, and 2) the dielectric constant. The two depletion layers can only be distinguished from each other by using EIS if the electrical time constants $\tau=C/G$ for each of the DL are sufficiently different. This EIS-detected difference in the nanocomposite membranes is immediately obvious from the EIS spectra, which show two clearly distinct dispersions with frequency.

In this work, we observed the formation of two differentiated parts of the depletion layer based on the different natures of the two layers forming the nanocomposite membranes. The positive region of the nanocomposite membranes is heterogeneous formed by polyethylene, polypropylene, and ion exchange resins. On the contrary, the positive layer is more homogeneous and is formed by sPPO and two nanomaterials, functionalized iron oxide nanoparticles and functionalized CNTs. These differences will almost certainly give rise to different dielectric constants, which means the depletion layers will most certainly be different.

The added negatively charged layer has an enhanced dielectric constant as this layer contains inorganic nanoparticles, such as the iron oxide nanoparticles, that are reported to have very high dielectric constant when compared to polymer matrixes [39]. In the case of the metallic nanoparticles, the dielectric constant of the nanoparticles themselves can be considered almost infinite [39]. Incorporation of multiwall carbon nanotubes in polymer matrixes has been reported to increase the dielectric constant more than 20 fold [40]. Thus, the dielectric constant of the negative region will be much higher than in the positive region. This difference in dielectric constant of the two layers in the composite membrane provides an explanation for the difference in capacitance observed in the two

parts of the total depletion layer, denoted as DL1 and DL2. At a given thickness, the capacitance will increase as the dielectric constant increases; thus, the depletion layer thickness itself increases with the increasing dielectric constant. DL1 is the depletion layer formed at the region with the highest dielectric constant, the nanocomposite layer; furthermore, the lower capacitance of this layer suggests that the depletion layer itself had a stronger than inverse linear dependence on the dielectric constant even though it has a higher dielectric constant. The effect of the Nernst potentials developed across the nanocomposite membrane further complicates the situation as this potential will also appear across the depletion layer. A more complete analysis of this is reserved for a future publication. DL2 is the depletion layer formed at the positive region.

A comparison of the capacitance and conductance of these two DLs in different solution concentrations will be discussed in the next section.

The influence of IEC (N^+ or N^- in Eq. 7 and 8) over the width of the depletion layer was not taken into account because the two regions had very similar fixed charge densities; IEC $1.8 \text{ meq}\cdot\text{g}^{-1}$ [33] for the positive region and $2.2 \text{ meq}\cdot\text{g}^{-1}$ [41] for the negative region.

Figure 6d) includes the ECC taking into account the underlying physical behavior that describes the electrical performance of nanocomposite AEMs. The difference between the ECC detected by EIS and the ECC in Figure 6d) is due to the fact that EIS only separates layers of different electrical time constants. The two layers that form the nanocomposite AEMs, although different in composition and charge, behave as a pure conductance in the presence of an alternating current. Thus, the parameter G_M corresponds to the sum of the conductance of the nanocomposite layer G_{M1} and the unmodified anion exchange membrane G_{M2} displayed in Figure 6d).

As a result of fitting the model to the EIS data, five parameters were obtained to describe the electrical behavior of the system; conductances G_M , G_{DL1} and G_{DL2} corresponding to the membrane, depletion layer DL1 and depletion layer DL2, and capacitances C_{DL1} and C_{DL2} corresponding to DL1 and DL2 respectively. The additional charge, caused by the introduction of the negatively charged layer on AEMs surface, is the reason behind the improved monovalent selectivity observed in the previous section *Analysis of monovalent ion permselectivity*. The change in membrane surface charge was also confirmed by ζ -potential measurements.

The parameters that describe DL1 and DL2 are closely related to the existence of the nanocomposite layer on the surface of nanocomposite AEMs. Thus, the periodical monitoring of these parameters during the operation of nanocomposite membranes can give valuable information about the stability of the layer. EIS was reported to be able to predict the fouling damage in membranes by monitoring changes in the membrane capacitance [30,42,43]. This way, EIS could also be a very useful tool for monitoring stability and fouling of layered ion-exchange membranes such as the nanocomposite membranes synthesized in this work.

3.2.3 Impedance of IEMs: influence of ion concentration

This section studies the influence of solution concentration over the electric behavior of IEMs. Figure 8 includes the changes in the impedance and capacitance of the nanocomposite membrane AM-0.4NP in four different solution concentrations: 0.01 mol·L⁻¹ of NaCl, 0.05 mol·L⁻¹ of NaCl, 0.1 mol·L⁻¹ of NaCl and 0.5 mol·L⁻¹ of NaCl. Overall, it is clear that the impedance decreased as the concentration of ions in the solution increased. The opposite trend is observed for the capacitance of the system. The capacitive character of the system increased as the ion concentration increased. The same influence of solution concentration over impedance and capacitance was observed for the other nanocomposite membrane AM-0.6CNTs.

For a better understanding of how ion concentration affects the system, Figure 9 and Figure 10 include the representation of the parameters of each layer, G_M , G_{DL1} , G_{DL2} , C_{DL1} and C_{DL2} , for the different solution concentrations and the different IEMs. A summary of the values for the G_M , G_{DL1} , G_{DL2} , C_{DL1} and C_{DL2} and the fitting parameter χ^2 and reduced χ^2 for the different concentration and IEMs is included in Table S1 of the supplementary data.

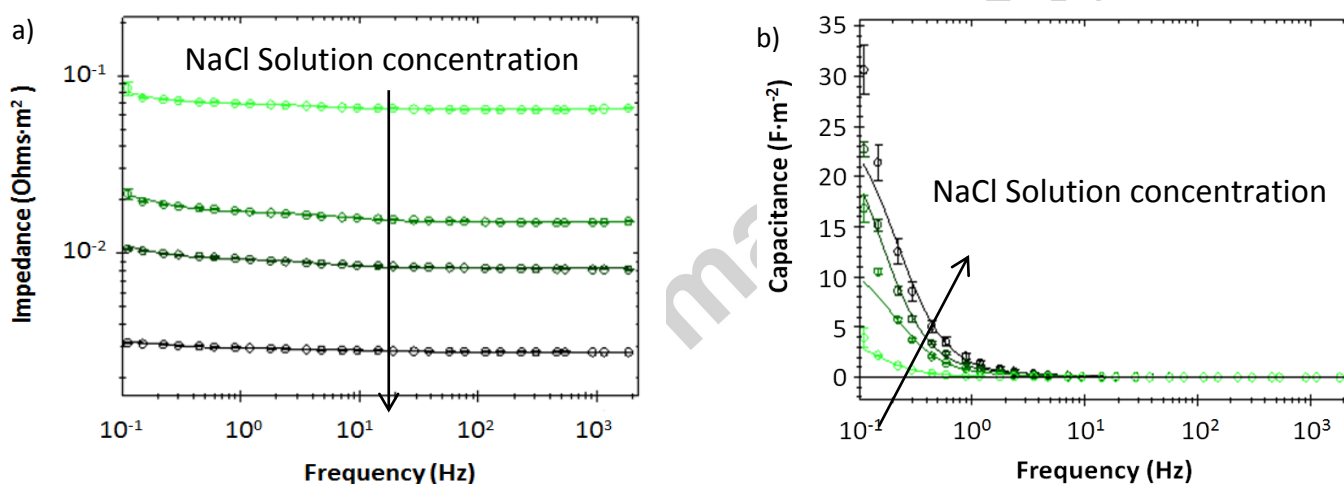


Fig 8. Evolution of a) impedance and b) capacitance with frequency for the membranes AM-0.4NP in solutions 0.01 mol·L⁻¹ of NaCl o, 0.05 mol·L⁻¹ of NaCl o, 0.1 mol·L⁻¹ of NaCl o and 0.5 mol·L⁻¹ of NaCl o. Maxell-Wagner fitting of the experimental data are shown as continuous lines. The error bars indicate the standard errors for three separate EIS spectra.

Figure 9 shows the conductance of IEMs G_M in the different solutions. The results of this figure confirm that the membrane conductance of the original AM-PP membranes was unaltered by the membrane treatment. This confirms the small influence of the layer over the total membrane resistance as already observed in our previous studies [28,29]. The membrane conductance increases with increasing solution concentration. This was observed previously in IEMs [17][21]. However, in this work we additionally observed a linear relationship between G_M and solution concentrations for all the studied membranes. A summary of the modeling of the influence of solution concentration on the electrical parameters of the proposed model is included in Table S2 of the supplementary data.

Figure 10a) shows the conductance G_{DL1} and G_{DL2} of DL1 and DL2. The conductance of DL1 and DL2 is an order of magnitude higher than the overall membrane conductance. Although the specific conductivity of the depletion layers is expected to be much smaller than that of the remainder of the membrane, the depletion layer is much thinner (nanometers) compared to the overall thickness of $\approx 500 \mu\text{m}$ of the nanocomposite AEM [28]. Thus if the conductance of each layer is calculated taking into account the thickness, also known as intrinsic conductance, it is clear that the conductance of the depletion layers is lower than the conductance of the membrane layer. The importance of thickness in comparing the electric resistance of membranes has been reported elsewhere [41]. The low conductance of depletion layers are due to the fact that these layers are almost completely depleted of mobile ions presenting a relatively high electrical resistance in comparison with other regions of the membrane where the counter-ions have a high concentration [35]. The conductance of depletion layers increases when increasing the solution concentration in a linear trend. The same is also true for the capacitance of both depletions layers (Figure 10b)). It can also be concluded that the depletion layer with the higher capacitance DL2 is also the one with the lowest conductance (Figure 10a)). Additionally, the main contribution to the capacitive behavior of the system arises from DL2, the depletion layer generated in the positive region in the interface between the membrane AM-PP and the nanocomposite layer.

The EIS measurements did not show significant differences between the two nanocomposite AEMs, AM-0.4NP and AM-0.6CNTs membranes, in the range of frequencies and solution concentrations used in this study. This finding is in line with the similarities in monovalent selectivity, Cl^- flux and ζ -potential discussed previously in the present work. In our previous study [28] we also showed close similarities in membrane roughness, water contact angle and fouling resistance.

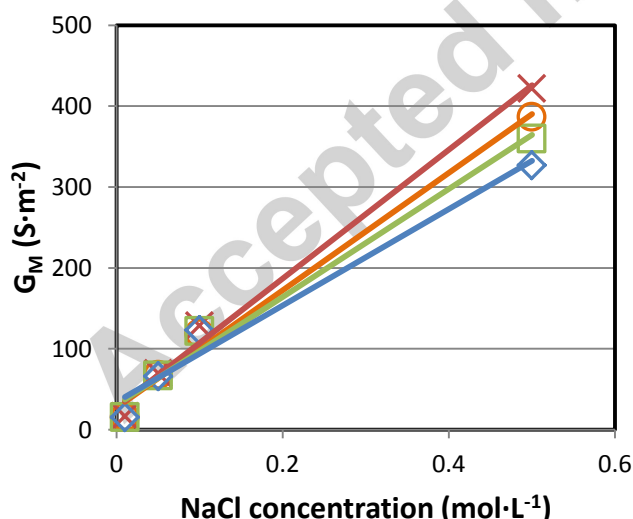


Fig 9. Membrane conductance G_M of membranes CM-PP X, AM-PP \circ , AM-0.4NP \square , and AM-0.6CNTs for \diamond different solution concentrations.

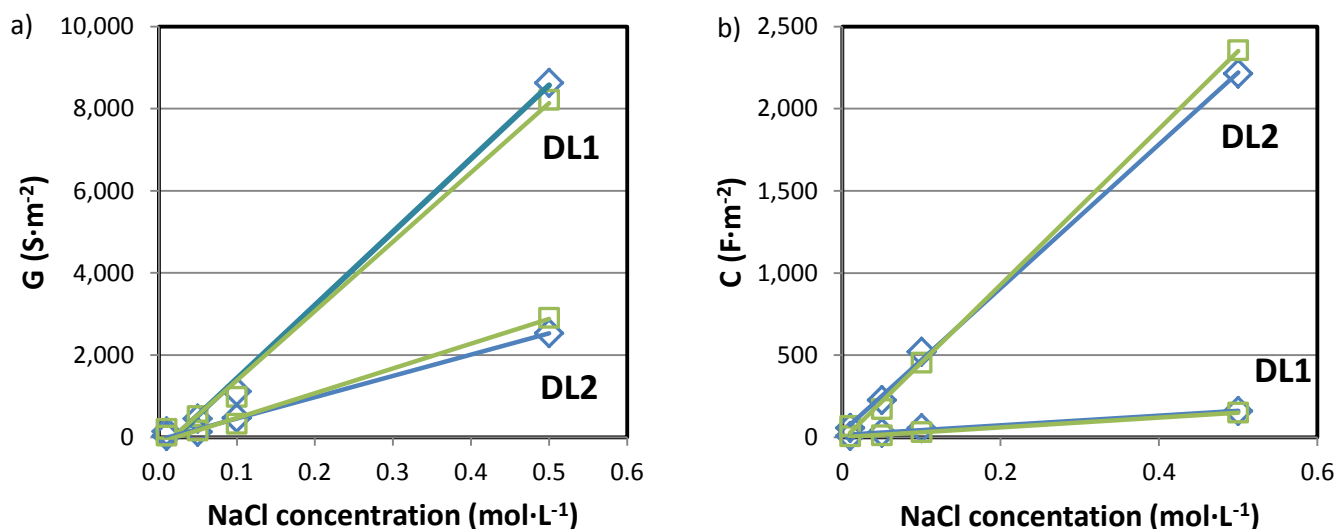


Fig 10.a) Conductance and b) capacitance of DL1 and DL2 of nanocomposite membranes AM-0.4NP \square and AM-0.6CNTs \diamond for different NaCl solution concentrations.

4. Conclusions

This work presents the enhancement of Cl^-/SO_4^{2-} mono-selectivity of layered nanocomposite AEMs and the mechanism that supports this improvement. These nanocomposite membranes are based on commercial polyethylene AEMs and a nanocomposite negative thin layer made of sPPO and different loadings of $Fe_2O_3-SO_4^{2-}$ nanoparticles or $CNTs-COO^-$, giving two different layers. The introduction of any of these two layers caused a change in the membrane surface charge that increased the electrostatic repulsions between sulfate and the membrane surface, providing nanocomposite membranes with better monovalent selectivity. The enhancement of the monovalent selectivity ranged from 26% to 34% and was maximum for the nanocomposite membranes AM-0.4NP and AM-0.6CNTs. Additionally the coating of the AEMs with the nanocomposite layer increased the flux of Cl^- up to 17% without losing Na^+/Cl^- permselectivity.

This is the first time that a simultaneous improvement of monovalent selectivity and Cl^- flux is reported in these types of layered membranes. ζ -potential and EIS measurements provided qualitative and quantitative evidence to support the change in the surface charge responsible for the improved monovalent selectivity. ζ -potential measurements showed that the surface charge of the AEMs changed from positive to negative with the coating (from 10 mV to -10 mV). EIS measurement showed that while unmodified membranes perform as a pure conductance in the presence of alternating currents, nanocomposite membranes present a combination of conductive and capacitive character. The fitting of the EIS data to a Maxwell-Wagner model showed that conventional IEMs can be basically described by one layer made with a pure

conductance under the experimental conditions used in this study. However, nanocomposite membranes need to be described by a combination of three layers. One layer corresponds to the pure conductance associated to the nanocomposite membranes. The remaining two layers were described by a combination of a conductance and a capacitance, identified as two parts of a depletion layer formed at the interface between the positive region and the negative region of the nanocomposite membranes. The two component depletion layers could be observed in the EIS measurements because they had distinctly different time constants. This, in turn, is probably the result of the differences in the dielectric constant between the two membrane regions arising from the nanomaterials incorporated in the negative region. The region of the membrane with the nanomaterials would be expected to have the higher dielectric constant. This ultimately translated into a thicker thickness of the depletion layer and lower capacitance, despite the fact that the capacitance would otherwise increase with an increasing dielectric constant. On the contrary, the positive region of nanocomposite membranes, with a significantly lower dielectric constant, resulted in a smaller depletion layer and dominated the total capacitive character of the nanocomposite membranes. The study of the ion concentration over EIS data showed that both conductance and capacitance of nanocomposite membranes displayed a linear trend with increasing concentration of the external solution.

This study has shown the importance of the new interface generated at the junction between the nanocomposite layers and the AEMs from an electrical point of view. This is the first time that depletion layers associated with this interface have been identified in advanced layered IEMs. This identification significantly adds to understanding of the electric nature of advanced layered membranes where negative layers and positive layers generate new interfaces.

EIS has been shown to be a powerful tool for monitoring the performance and stability of layered nanocomposite membranes. The capacitive character of nanocomposite membranes is expected to disappear as the nanocomposite layer is damaged. This can be applied not only to the nanocomposite membranes studied herein, but also to all layered membranes where positive regions coexist with negative regions generating interfaces where depletion layers are formed in the presence of alternating currents.

Acknowledgments

Financial support from MICINN under project CTM2014-57833-R and CTQ2013-48280-C3-1-R-D is gratefully acknowledged. The authors thank the Ministry of Education for the FPI grant BES-2012-053461 and the scholarships EEBB-I-15-10268 and EEBB-I-16-11614. In addition, this research was partially supported by the U.S. National Science Foundation CBET-1235166.

References

- [1] R. Femmer, M.C. Martí-Calatayud, and M. Wessling. Mechanistic modeling of the dielectric impedance of layered membrane architectures. *J.Membr.Sci.*, 520 (2016) 29-36.
- [2] C. Fernandez-Gonzalez, A. Dominguez-Ramos, R. Ibañez, and A. Irabien. Electrodialysis with bipolar membranes for valorization of brines. *Separation and Purification Reviews*, 45 (2016) 275-287.
- [3] T. Sata. Studies on anion exchange membranes having permselectivity for specific anions in electrodialysis — effect of hydrophilicity of anion exchange membranes on permselectivity of anions. *J.Membr.Sci.*, 167 (2000) 1-31.
- [4] V.D. Grebenyuk, R.D. Chebotareva, S. Peters, and V. Linkov. Surface modification of anion-exchange electrodialysis membranes to enhance anti-fouling characteristics. *Desalination*, 115 (1998) 313-329.
- [5] T. Sata, T. Yamaguchi, and K. Matsusaki. Effect of hydrophobicity of ion exchange groups of anion exchange membranes on permselectivity between two anions. *J.Phys.Chem.*, 99 (1995) 12875-12882.
- [6] T. Sata, T. Yamaguchi, K. Kawamura, and K. Matsusaki. Transport numbers of various anions relative to chloride ions in modified anion-exchange membranes during electrodialysis. *Journal of the Chemical Society - Faraday Transactions*, 93 (1997) 457-462.
- [7] T. Sata, K. Mine, and M. Higa. Change in permselectivity between sulfate and chloride ions through anion exchange membrane with hydrophilicity of the membrane. *J.Membr.Sci.*, 141 (1998) 137-144.
- [8] T. Sata, Y. Tagami, and K. Matsusaki. Transport properties of anion-exchange membranes having a hydrophobic layer on their surface in electrodialysis. *J Phys Chem B*, 102 (1998) 8473-8479.
- [9] S. Mikhaylin, L. Bazinet. Fouling on ion-exchange membranes: Classification, characterization and strategies of prevention and control. *Adv.Colloid Interface Sci.*, 229 (2016) 34-56.
- [10] S. Mulyati, R. Takagi, A. Fujii, Y. Ohmukai, T. Maruyama, and H. Matsuyama. Improvement of the antifouling potential of an anion exchange membrane by surface modification with a polyelectrolyte for an electrodialysis process. *J.Membr.Sci.*, 417-418 (2012) 137-143.
- [11] M. Wang, X. Wang, Y. Jia, and X. Liu. An attempt for improving electroalytic transport properties of a heterogeneous anion exchange membrane. *Desalination*, 351 (2014) 163-170.
- [12] S. Mulyati, R. Takagi, A. Fujii, Y. Ohmukai, and H. Matsuyama. Simultaneous improvement of the monovalent anion selectivity and antifouling properties of an anion exchange membrane in an electrodialysis process, using polyelectrolyte multilayer deposition. *J Membrane Sci*, 431 (2013) 113-120.

- [13] M. Vasselbehagh, H. Karkhanechi, R. Takagi, and H. Matsuyama. Surface modification of an anion exchange membrane to improve the selectivity for monovalent anions in electro dialysis - experimental verification of theoretical predictions. *J.Membr.Sci.*, 490 (2015) 301-310.
- [14] E. Güler, W. van Baak, M. Saakes, and K. Nijmeijer. Monovalent-ion-selective membranes for reverse electro dialysis. *J.Membr.Sci.*, 455 (2014) 254-270.
- [15] R. Takagi, M. Vasselbehagh, and H. Matsuyama. Theoretical study of the permselectivity of an anion exchange membrane in electro dialysis. *J.Membr.Sci.*, 470 (2014) 486-493.
- [16] G.M. Geise, M.A. Hickner, and B.E. Logan. Ionic resistance and permselectivity tradeoffs in anion exchange membranes. *ACS Appl.Mater.Interfaces*, 5 (2013) 10294-10301.
- [17] W. Zhang, J. Ma, P. Wang, Z. Wang, F. Shi, and H. Liu. Investigations on the interfacial capacitance and the diffusion boundary layer thickness of ion exchange membrane using electrochemical impedance spectroscopy. *J.Membr.Sci.*, 502 (2016) 37-47.
- [18] J. Park, J. Choi, J. Woo, and S. Moon. An electrical impedance spectroscopic (EIS) study on transport characteristics of ion-exchange membrane systems. *J.Colloid Interface Sci.*, 300 (2006) 655-662.
- [19] V.V. Nikonenko, A.E. Kozmai. Electrical equivalent circuit of an ion-exchange membrane system. *Electrochim.Acta*, 56 (2011) 1262-1269.
- [20] W. Zhang, P. Wang, J. Ma, Z. Wang, and H. Liu. Investigations on electrochemical properties of membrane systems in ion-exchange membrane transport processes by electrochemical impedance spectroscopy and direct current measurements. *Electrochim.Acta*, 216 (2016) 110-119.
- [21] P. Dlugolecki, P. Ogonowski, S.J. Metz, M. Saakes, K. Nijmeijer, and M. Wessling. On the resistances of membrane, diffusion boundary layer and double layer in ion exchange membrane transport. *J.Membr.Sci.*, 349 (2010) 369-379.
- [22] D. Golubenko, Y. Karavanova, and A. Yaroslavtsev. Effects of the surface layer structure of the heterogeneous ion-exchange membranes on their impedance. *J Electroanal Chem*, 777 (2016) 1-7.
- [23] P. Sizat, A. Kozmai, N. Pismenskaya, C. Larchet, G. Pourcelly, and V. Nikonenko. Low-frequency impedance of an ion-exchange membrane system. *Electrochim.Acta*, 53 (2008) 6380-6390.
- [24] E.K. Zholkovskij. Irreversible Thermodynamics and Impedance Spectroscopy of Multilayer Membranes. *J.Colloid Interface Sci.*, 169 (1995) 267-283.
- [25] S. Abdu, M.-. Martí-Calatayud, J.E. Wong, M. García-Gabaldón, and M. Wessling. Layer-by-layer modification of cation exchange membranes controls ion selectivity and water splitting. *ACS Appl.Mater.Interfaces*, 6 (2014) 1843-1854.
- [26] J.G. Hong, Y. Chen. Nanocomposite reverse electro dialysis (RED) ion-exchange membranes for salinity gradient power generation. *J.Membr.Sci.*, 460 (2014) 139-147.

- [27] J. Gi Hong, Y. Chen. Evaluation of electrochemical properties and reverse electrodialysis performance for porous cation exchange membranes with sulfate-functionalized iron oxide. *J.Membr.Sci.*, 473 (2015) 210-217.
- [28] C. Fernandez-Gonzalez, B. Zhang, A. Dominguez-Ramos, R. Ibañez, A. Irabien, and Y. Chen. Enhancing fouling resistance of polyethylene anion exchange membranes using carbon nanotubes and iron oxide nanoparticles. *Desalination*, 411 (2017) 19-27.
- [29] C. Fernandez-Gonzalez, A. Dominguez-Ramos, R. Ibañez, Y. Chen, and A. Irabien. Valorization of desalination brines by electrodialysis with bipolar membranes using nanocomposite anion exchange membranes. *Desalination*, 406 (2017) 16-24.
- [30] J. Cen, M. Vukas, G. Barton, J. Kavanagh, and H.G.L. Coster. Real time fouling monitoring with Electrical Impedance Spectroscopy. *J.Membr.Sci.*, 484 (2015) 133-139.
- [31] L. Gaedt, T.C. Chilcott, M. Chan, T. Nantawisarakul, A.G. Fane, and H.G.L. Coster. Electrical impedance spectroscopy characterisation of conducting membranes II. *Experimental J.Membr.Sci.*, 195 (2002) 169-180.
- [32] H.G.L. Coster, T.C. Chilcott, and A.C.F. Coster. Impedance spectroscopy of interfaces, membranes and ultrastructures. *Bioelectrochem.Bioenerget.*, 40 (1996) 79-98.
- [33] R. Ibañez, A. Pérez-González, P. Gómez, A.M. Urtiaga, and I. Ortiz. Acid and base recovery from softened reverse osmosis (RO) brines. Experimental assessment using model concentrates. *Desalination*, 309 (2013) 165-170.
- [34] N. Pismenskaya, N. Melnik, E. Nevakshenova, K. Nebavskaya, and V. Nikonenko. Enhancing ion transfer in overlimiting electrodialysis of dilute solutions by modifying the surface of heterogeneous ion-exchange membranes. *Int.J.Chem.Eng.*, (2012).
- [35] H.G. Coster. The double fixed charge membrane. Low frequency dielectric dispersion. *Biophys.J.*, 13 (1973) 118-132.
- [36] A. Mauro. Space Charge Regions in Fixed Charge Membranes and the Associated Property of Capacitance. *Biophys.J.*, 2 (1962) 179-198.
- [37] H.G.L. Coster. A Quantitative Analysis of the Voltage-Current Relationships of Fixed Charge Membranes and the Associated Property of "Punch-Through". *Biophys.J.*, 5 (1965) 669-686.
- [38] H.G.L. Coster. The Double Fixed Charge Membrane: Solution-Membrane Ion Partition Effects and Membrane Potentials. *Biophysical Journal*, 13 (1973) 133-142.
- [39] L. Zhu. Exploring strategies for high dielectric constant and low loss polymer dielectrics. *J.Phys.Chem.Lett.*, 5 (2014) 3677-3687.
- [40] L. Wang, Z.-. Dang. Carbon nanotube composites with high dielectric constant at low percolation threshold. *Appl.Phys.Lett.*, 87 (2005).
- [41] X. Tong, B. Zhang, and Y. Chen. Fouling resistant nanocomposite cation exchange membrane with enhanced power generation for reverse electrodialysis. *J.Membr.Sci.*, 516 (2016) 162-171.

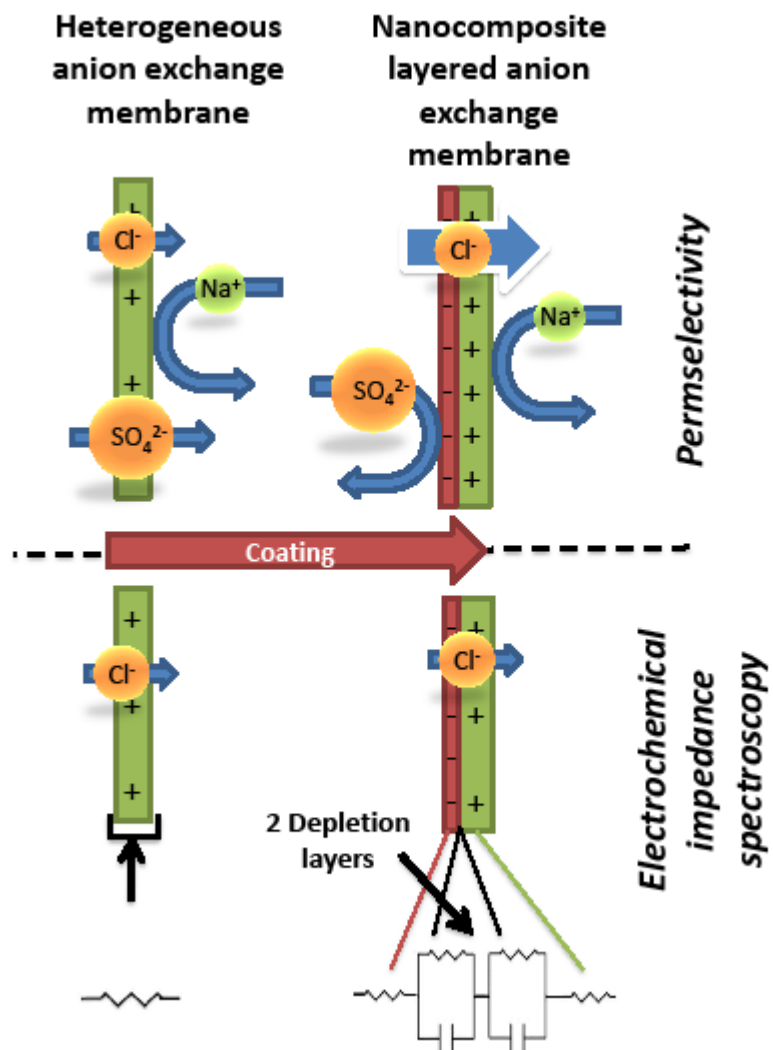
[42] J.M. Kavanagh, S. Hussain, T.C. Chilcott, and H.G.L. Coster. Fouling of reverse osmosis membranes using electrical impedance spectroscopy: Measurements and simulations. *Desalination*, 236 (2009) 187-193.

[43] J. Cen, J. Kavanagh, H. Coster, and G. Barton. Fouling of reverse osmosis membranes by cane molasses fermentation wastewater: Detection by electrical impedance spectroscopy techniques. *Desalin. Water Treat.*, 51 (2013) 969-975.

Highlights

- EIS was applied to tailor-made layered nanocomposite membranes
- An equivalent electric circuit based on the Maxwell-Wagner model was applied
- The equivalent electric circuit is related to the structure of the layered membranes
- Differences in dielectric constant in the layered membrane influence depletion layers
- Layered nanocomposite membrane stability can be easily assessed by EIS

Accepted manuscript



Graphical Abstract